Isolated rigid rod behavior of functionalized single-wall carbon nanotubes in solution determined via small-angle neutron scattering

A. Urbina* and C. Miguel
Dep. de Electrónica, Universidad Politécnica de Cartagena, 30202-Cartagena, Spain

J. L. Delgado and F. Langa
Facultad de Ciencias del Medio Ambiente, Universidad de Castilla-La Mancha, 45071-Toledo, Spain

C. Díaz-Paniagua
Centro Español de Metrología, Tres Cantos, 28760 Madrid, Spain

F. Batallán
Instituto de Ciencia de Materiales de Madrid, CSIC, Cantoblanco, 28049 Madrid, Spain
(Received 29 January 2008; revised manuscript received 7 May 2008; published 21 July 2008)

The measurement of small-angle neutron scattering on functionalized single-wall carbon nanotubes in solution is reported. Without the use of surfactants, isolated rigid rod behavior of functionalized single-wall carbon nanotubes has been observed. The onset of pinning between the nanotubes at different pinning distances depending on the concentration is also detected, as well as some aggregation for the more concentrated samples. We present evidence of a multiscale organization of these samples: the molecular covalent structure of single-wall nanotubes, the supramolecular structure of bundles, and a loose three-dimensional network formed by pinning of the bundles. Since most organic electronic devices are fabricated from blends of small molecules or nanocrystals with a polymeric matrix by spin coating from solution, the understanding of the solution properties of such nanocrystals is important in order to improve the performance of these devices.

DOI: 10.1103/PhysRevB.78.045420 PACS number(s): 61.46.Fg, 61.05.fd, 61.46.Km, 61.48.De

I. INTRODUCTION

The new molecular forms of sp^2 hybridized carbon—fullerenes and nanotubes—are two of the most thrilling materials which have been developed in recent decades. Carbon nanotubes (CNTs)[1] hold great promise as an ideal low-weight carbon fiber with mechanical[2] and electronic transport properties[3,4] that make them ideal candidates for molecular wires. From an electronic point of view, carbon nanotubes are semiconducting or metallic materials, depending on the chirality of the nanotube. This property is a great advantage, but also becomes a problem if we cannot select and assemble nanotubes of different kinds as desired, especially when the devices are made with a bottom-up approach such as with the new organic molecular electronic devices, which are created from blends of conjugated polymers (usually semiconducting *p*-type materials) and carbon nanotubes (ideally metallic or semiconducting *n*-type materials). They are the so-called "bulk heterojunction" devices,[5] mainly used to develop organic light emitting diodes and organic photovoltaic cells.[6]

The performance of such devices depends strongly on the nanostructure of the interpenetrated networks of both kinds of materials. The configuration of distances between rods, distances between inter-rod pinning points, and stability of the networks created from the rods in solution will determine the properties of the final blend. The study of the solution (or suspension) phase of these materials is crucial to understanding the self-organization processes, which will ultimately allow us to control the large-scale industrial fabrication of the devices. Hence, a better understanding of the morphology of such solutions is needed in order to improve the control of these solution-based fabrication methods.

Bulk material containing carbon nanotubes has been characterized by Rols *et al.*[7–9] in neutron scattering experiments, which studies the vibrational properties of CNTs. These measurements have been performed on solid samples of self-assembled nanobundles of single-wall nanotubes (SWNT) using inelastic neutron scattering at low energies (0 to 225 meV). Good agreement between the calculated phonon density of states and experimental results for the SWNT lattice over the entire energy range was found. Also small-angle neutron scattering (SANS) results were presented for SWNT dilute suspensions in water using surfactants, where, after considerable data treatment in order to eliminate the surfactant signal, evidence for isolated rigid rods and rod networks has been shown.[10–12] We have also performed previous neutron scattering experiments in samples of carbon nanotubes-dissolved in deuterated toluene using incoherent elastic neutron scattering (IENS) and incoherent quasielastic neutron scattering (IQNS) techniques in the temperature range between 4 and 300 K. Three phases were observed by IENS measurements: a solid phase for $T<T_g$, an undercooled liquid phase for $T_g<T<T_m$, and a liquid phase for $T>T_m$. Three different quasielastic peaks were identified, two in the liquid phase and another one in the undercooled liquid phase.[13]

We shall now proceed to report SANS measurements of stable solutions of functionalized single-wall carbon nanotubes in deuterated toluene at room temperature. We functionalized the SWNTs with pentyl ester groups at the ends. This functionalization allowed both to get stable solutions

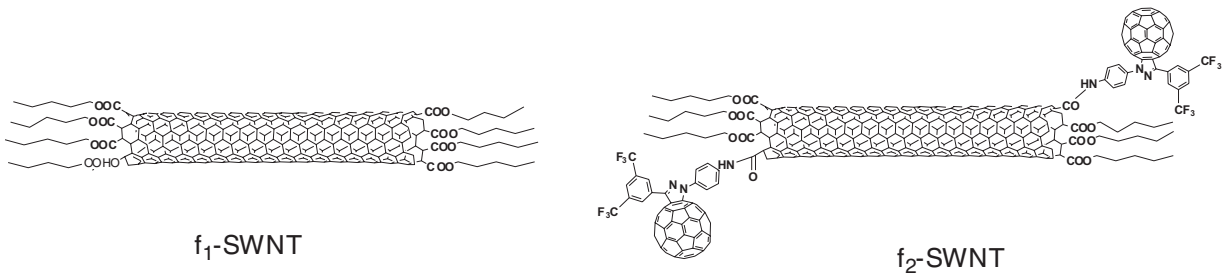

FIG. 1. Schematic draft of the molecular structure of both functionalized single-wall carbon nanotubes: f_1 SWNT is the pentyl-ester SWNT and f_2 SWNT is the conjugated hybrid of C_{60}-fullerene and SWNT.

and to enhance the neutron scattering signal by protonation of the sample dissolved in a deuterated solvent (toluene).

II. SAMPLE PREPARATION AND CHARACTERIZATION

Carbon nanotubes have been a difficult material to handle, especially when they have to be processed in solution or suspension. Special attention has been paid to prepare soluble derivatives of carbon nanotubes using chemical procedures which do not destroy the excellent mechanical and electrical properties of the nanotubes. Furthermore, avoiding the use of surfactants in the sample preparation procedure overcomes the problem of subsequent purification if this material is to be used in optoelectronic applications, where a small amount of contaminants will quench the desired performance of the fabricated devices.

We have prepared functionalized single-wall carbon nanotubes that enable us to get stable solutions without the use of surfactants. Our samples were prepared starting from acid purified HiPCO SWNTs, at the end of which were carboxylic groups that were reacted first with thionyl chloride and then by addition of *n*-pentanol. This resulted in *n*-pentyl ester groups attached at the ends of the nanotubes, which make them soluble in toluene. This sample is named f_1 SWNT in Fig. 1. f_1 SWNT was characterized by means of nuclear magnetic resonance (1H-NMR), ultraviolet-visible (UV-vis) absorption spectroscopy, and Fourier transform infrared spectroscopy (FTIR). More sample preparation and characterization details are given in the references.[14,15] A sample with a slightly different functionalization (f_2 SWNT in Fig. 1), including a fullerene derivative, was also prepared. This material is the synthesis of a conjugated hybrid of C_{60} fullerene and a single-wall carbon nanotube. The new nanohybrid material was prepared by amidation reaction between a carboxylic single-wall carbon nanotube (SWCNT) and an aniline-fullerene derivative. Characterization of the sample was performed by means of attenuated total reflectance Fourier infrared spectroscopy (ATR/FTIR) and Raman spectroscopy.[16]

In Fig. 2 we show a high-resolution transmission electron microscopy (HRTEM) image of f_2 SWNT that was taken with a JEOL JEM-4000 EX transmission electron microscope, operated at 250 kV and equipped with a field emission gun (FEG), which enabled us to achieve a point resolution of 0.2 nm. An individual functionalized carbon nanotube can be seen, as well as some aggregations of nanotubes to create a bundle. Both are characteristic of the particles in the solution: individual carbon nanotubes and bundles of about 10 nm in diameter. Since it is difficult to obtain a well-defined rate of individual to bundled nanotubes, we will call them collectively "rigid rods" because they can be considered as isolated rodlike nanostructures with a huge length-to-width ratio. For the neutron scattering experiments, solutions of the nanotubes in deuterated toluene at different weight concentrations were prepared. The weight concentrations of functionalized nanotubes (f_1 SWNT) in deuterated toluene were 0.025%, 0.1%, and 0.4% wt. For samples above a critical density of about 0.5% wt, the aggregation increases strongly and it triggers precipitation in a few hours. Finally, a sample with the second functionalization (f_2 SWNT) was prepared. In this case, solubility is lower and the maximum concentration that we could obtain was 0.05% wt. The interest of this last sample is its possible application to organic optoelectronic devices since the C_{60} is a strong electron acceptor and improves the exciton dissociation and charge collection for a more efficient photocurrent generation in organic solar cells.

III. SMALL-ANGLE NEUTRON SCATTERING MEASUREMENTS: RESULTS AND DISCUSSION

We used three different configurations of the small-angle neutron scattering D11 instrument at Institute Laue Langevin

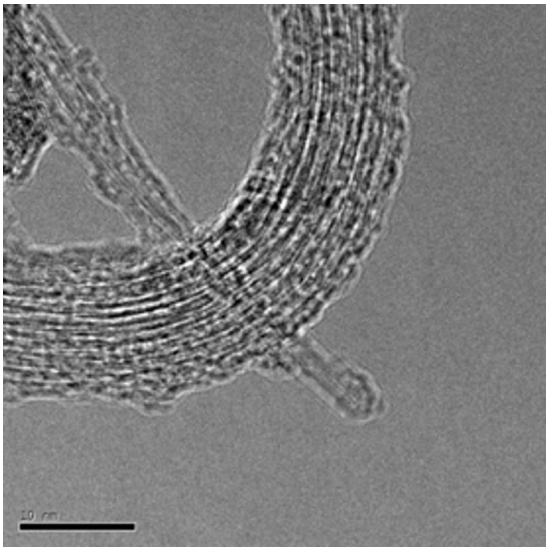

FIG. 2. HRTEM image of a functionalized carbon nanotube and a bundle of nanotubes. The diameters of nanotubes are of 1.5 nm, and those of bundles are of around 10 nm (bar: 10 nm).

TABLE I. Instrumental parameters for the large-angle (LA), medium-angle (MA), and small-angle (SA) configurations used in our neutron scattering measurements.

	LA	MA	SA
sample-detector distance (m)	1.1	5	14
collimator distance (m)	1.5	16.5	40.5
$Q_{\min}$(Å^{-1}) (r=6 cm)	5.71×10^{-2}	1.26×10^{-2}	4.49×10^{-3}

(ILL). The configurations are, respectively, called small angle (SA), medium angle (MA) and large angle (LA), as indicated in Table I. This allowed us to explore a wide range of the scattering vector Q, with enough overlapping between the configurations, so a superposition of different spectra in the same plot was easily obtained. All measurements were performed at room temperature. We used an incident neutron wavelength of 6 Å and a sample aperture of 0.7 cm^2. Raw data were corrected for electronic background and empty cell, and normalized in absolute scale using water scattering and standard instrument software.[17]

In Fig. 3 we show graphs with a log-log plot of $I(Q)$ vs Q for the different concentrations of carbon nanotubes. The different measurement configurations (SA, MA, and LA) are plotted for every sample, showing a good overlapping between them. The measured absolute intensities are low (below 1 cm^{-1}) because of the low concentration of scattering centers in our samples. In the lowest concentration plot, the pure deuterated toluene measurement was superimposed to indicate the range of Q values where the solvent damps the behavior of the sample. We can obtain straightforward log-log plots of the rods signal without any surfactant subtraction. The deuterated toluene shows a flat behavior and does not affect the different Q dependences discussed in the next paragraphs. It can be observed that the plots are composed of different regions with $I(Q)=aQ^{-\alpha}$, with α defining a different characteristic power law for every region. All samples show a range of Q^{-1} behavior, which is indicative of the presence of isolated rigid rods since the scattered intensity for isolated rigid rods follows a Q^{-1} behavior for a wave-vector range given by $2\pi/L<Q<2\pi/D$, where D is the diameter and L the length of the rods.[18,19] The limits of this range can be obtained from the plots, as it is shown in more detail in Fig. 4 for the SA scattering configuration.

A characteristic length, L, can be calculated from the lower Q limit of the transition. The concentration dependence of this length is indicated in Table II, where it can be seen that the obtained values are strongly dependent on concentration with a clear inverse trend. For the lowest concentration there was no Q^{-1} behavior, and hence the method is not applicable for this sample. Since we do not have enough different values, no dependence law can be envisaged.

The upper limit for the Q^{-1} behavior cannot be clearly defined since the signal is very low and the solvent begins to be significant for a Q value at the onset of the medium-angle instrumental configuration (indicated by an horizontal segment in Fig. 4).

For lower Q values, the obtained power law gives $-3<\alpha<-2$, with a slight variation depending on the concentration of nanotubes. This is consistent with the hypothesis that if a number of rods are brought together, they can form an aggregate and the power law associated with such a structure should be between −2 and −3, depending on the type of pinning between the rods.[20] The obtained power law strongly suggest aggregation in our samples. On the other hand, a power law of $-5/3$ is characteristic of a semiflexible chain,

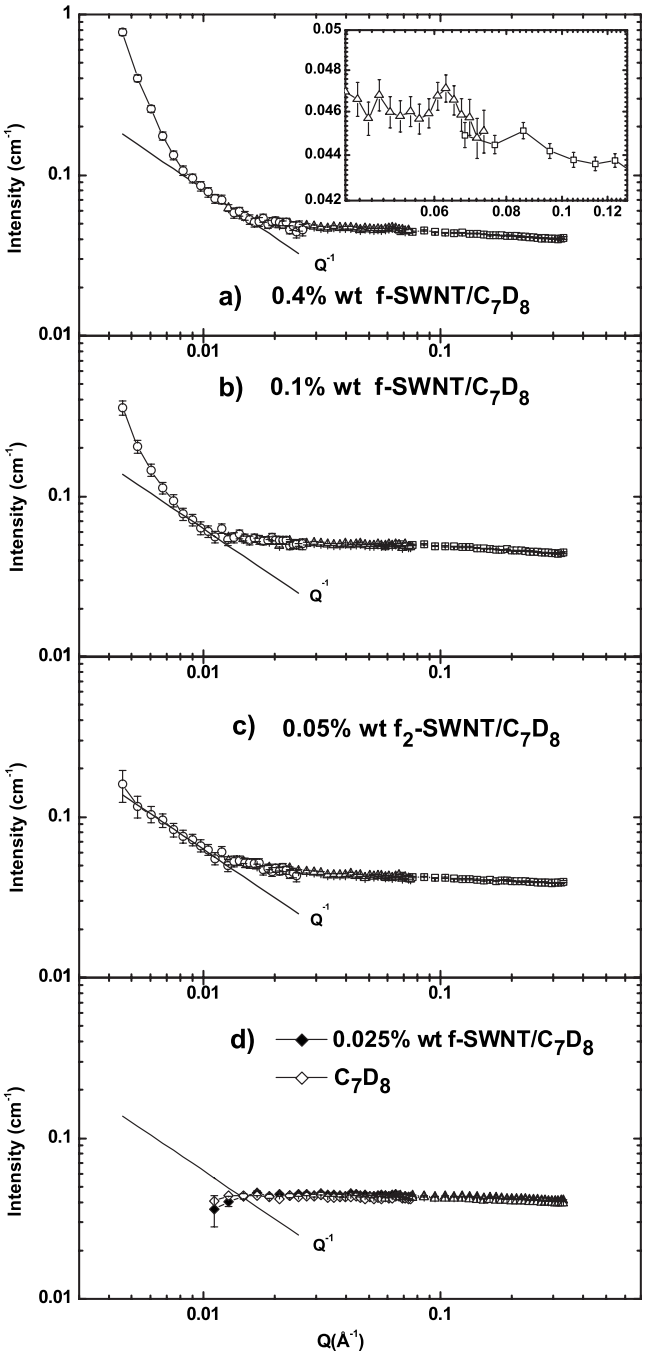

FIG. 3. SANS intensity profiles for pentyl-ester single-wall carbon nanotubes dissolved in deuterated toluene at 0.4, 0.1, 0.05, and 0.025% wt. The plot includes the three instrumental configurations used: small (circles), medium (triangles), and large (squares) angles. No solvent subtraction was performed. We can see a clear Q^{-1} behavior over a wide range of Q values. In addition the signal from deuterated toluene is plotted for comparison.

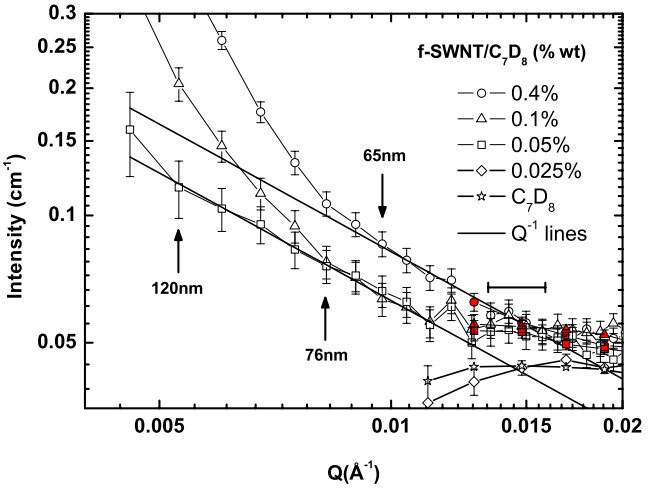

FIG. 4. (Color online) Detail of the small-angle scattering measurement for all the samples. The lower Q limit for every sample is pointed by an arrow. The corresponding number indicates the pinning distance deduced from this limit. The horizontal segment indicates the onset of the solvent signal in the plot, which terminates the Q^{-1} behavior without reaching its theoretical limit deduced from the diameter of the SWNTs. Filled symbols are medium-angle configuration measurements.

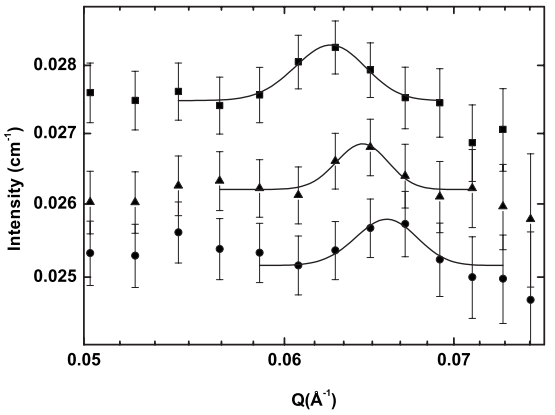

FIG. 5. Detail of the medium-angle scattering measurement for three samples: 0.4 and 0.1% wt of f_1 SWNT (squares and triangles) and 0.05% wt f_2 SWNT (circles) corrected by solvent subtraction. The observed peaks have been fitted with a Gaussian function (lines).

which could suggest the presence of long semiflexible nanotubes. Such behavior is not observed in our samples so we discard the presence of long isolated nanotubes. Power laws between −2 and −3 could also be associated with objects of a large flat disk shape, but it is unlikely that SWNT aggregations could form such objects. A stable range of Q^{-2} behavior could be an indication of a loose three-dimensional (3D) network, similar to semidilute phases of flexible polymer solutions, where the mesh size approaches the polymer persistence length as suggested by de Gennes.[21] In a simplified model of a 3D network of rigid rods, the expected length scale for the crossover between Q^{-1} and Q^{-2} behavior should be comparable to the average distance of the pinning points between the rods, and only rods with lengths smaller than this distance can be seen as isolated rods. The average distance of the pinning points for the 3D network depends on the concentration of nanotubes. Hence, for higher concentrations, the obtained distance is lower.

Finally we would like to present the behavior of the signal at larger Q values. In this result the solvent signal is important, but it presents a flat contribution [see Fig. 2(d), C_7D_8 signal], and therefore does not modify the location of the observed features. Some peaks, well above the noise level, are observed in all samples for intermediate Q values, as shown in the inset of the plot corresponding to the 0.4% wt sample in Fig. 3(a). It is worth mentioning the clear wide peak observed at $Q=0.062$ Å^{-1} for this high weight-concentration sample. This Q value corresponds to a limiting value for the diameter of the rods at a characteristic length of about $2\pi/0.06 \sim 10$ nm, which is the diameter of a typical bundle of nanotubes (in good agreement with what is observed in Fig. 2). We can therefore attribute this feature to some rod-rod correlation. In order to perform a more detailed analysis, we present in Fig. 5 a plot where the scattering signal from the samples has been corrected by subtracting the solvent contribution. This procedure increases the error bars until an uncertainty of about 8.5%. Nevertheless, we can now clearly appreciate a peak in the three samples of higher nanotube concentration. The intensity of these peaks reduces for lower concentration samples and cannot be detected in the 0.025% wt sample. We have fitted the peaks to a Gaussian function, using an instrumental weight for the data points given by $w_{ij}=1/\sigma_{ij}^2$, where σ_{ij} are the error bars of the measurements. The results of the fitting are presented in Table III: there is a slight displacement of the center of the peak from 0.0626 Å^{-1} for the 0.4% wt sample to 0.0659 Å^{-1} for the 0.05% wt sample. A reduction in the intensity of the peak (height above offset value) from the higher- to the lower-concentration sample can also be observed. These facts are consistent with the above-mentioned explanation of the aggregation of the nanotubes in bundles of about 10 nm diameter. It could also explain the shorter range of Q^{-1} behavior in the 0.4% wt sample since the aggregation effect damps the signal from isolated nanotubes. Further measurements for different concentrations of nanotubes in the solution should be performed in order to clarify this point.

TABLE II. Lower Q values for the Q^{-1} ranges measured for the different carbon nanotube concentration and the calculated corresponding length from the onset of the Q^{-1} behavior as explained in the text.

SWNT % wt	lower Q limit (Å^{-1})	L (nm)
0.4	0.0097	65
0.1	0.0082	76
0.05	0.0053	120

IV. CONCLUSIONS

In summary, we have prepared stable solutions of functionalized single-wall carbon nanotubes in deuterated tolu-

TABLE III. Fitting parameters of the Gaussian functions used to fit the observed medium-angle scattering peaks (lines in Fig. 5). The samples are the 0.4%wt and 0.1%wt f_1-SWNT, and 0.05% wt f_2-SWNT.

Sample % wt:	0.4%	0.1%	0.05%
Center ($Å^{-1}$)	0.0626	0.0644	0.0659
Bundle diameter (nm)	10.05 ± 0.85	9.76 ± 0.85	9.53 ± 0.85
Height (10^{-4} cm^{-1})	8.292	6.491	6.311
Width ($Å^{-1}$)	0.00397	0.00299	0.00365
Offset (cm^{-1})	0.0275	0.0262	0.0251
χ^2/DoF	0.04227	0.05748	0.10224
corr. coeff.	0.95853	0.90379	0.82957

ene. These samples were carefully characterized, and the solutions enabled us to perform small-angle neutron scattering measurements without the use of surfactants at room temperature. Our analysis of the SANS measurements of functionalized single-wall carbon nanotube solutions indicates that they form an aggregate of rigid rods, pinned between themselves, creating a rigid 3D network with a characteristic distance between pinning centers, depending on the carbon nanotube concentration. This distance ranges between 120 and 65 nm. For solutions with a low concentration of nanobubes, a range of isolated rigid rod behavior with Q^{-1} power-law dependence could be observed. These samples display a multiscale organization: the molecular covalent structure of the single-wall nanotubes, the supramolecular structure of bundles with a diameter around 10 nm created by aggregation of nanotubes, and finally a loose three-dimensional network formed by pinning of the bundles.

ACKNOWLEDGMENTS

The authors thank Isabelle Grillo and Mónica Jiménez (Institute Laue Langevin) for their very helpful scientific and technical comments. We acknowledge the financial support from Ministerio de Educación y Ciencia (Spain) under Grants No. MAT2006-1270-C02-02, No. CTQ2007–63363, and Project No. HOPE CSD2007–00007 (Consolider Ingenio 2010).

*antonio.urbina@upct.es

[1] S. Iijima, Nature (London) **354**, 56 (1991).
[2] L. S. Schadler, S. C. Giannaris, and P. M. Ajayan, Appl. Phys. Lett. **73**, 3842 (1998).
[3] S. Frank, P. Poncharal, Z. L. Wang, and W. A. de Heer, Science **280**, 1744 (1998).
[4] A. Urbina, I. Echeverría, A. Pérez-Garrido, A. Díaz-Sánchez, and J. Abellán, Phys. Rev. Lett. **90**, 106603 (2003).
[5] G. Yu, J. Gao, J. Hummelen, F. Wudl, and A. J. Heeger, Science **270**, 1789 (1995).
[6] E. Kymakis, I. Alexandrou, and G. A. J. Amaratunga, J. Appl. Phys. **93**, 1764 (2003).
[7] S. Rols, E. Anglaret, J. L. Sauvajol, G. Coddens, and A. Dianoux, Appl. Phys. A: Mater. Sci. Process. **69**, 591 (1999).
[8] S. Rols, Z. Benes, E. Anglaret, J. L. Sauvajol, P. Papanek, J. E. Fischer, G. Coddens, H. Schober, and A. J. Dianoux, Phys. Rev. Lett. **85**, 5222 (2000).
[9] J. L. Sauvajol, E. Anglaret, S. Rols, and L. Alvarez, Carbon **40**, 1697 (2002).
[10] W. Zhou, M. F. Islam, H. Wang, D. L. Ho, A. G. Yodh, K. I. Winey, and J. E. Fisher, Chem. Phys. Lett. **384**, 185 (2004).
[11] H. Wang, W. Zhou, D. L. Ho, K. I. Winey, J. E. Fischer, C. J. Glinka, and E. K. Hobbie, Nano Lett. **4**, 1789 (2004).
[12] K. Yurekli, C. A. Mitchell, and R. Krishnamoorti, J. Am. Chem. Soc. **126**, 9902 (2004).
[13] A. Urbina, C. Miguel, J. L. Delgado, F. Langa, C. Díaz-Paniagua, M. Jiménez, and F. Batallán, J. Phys.: Condens. Matter **20**, 104208 (2008).
[14] M. Alvaro, P. Atienzar, P. la Cruz, J. L. Delgado, H. García, and F. Langa, Chem. Phys. Lett. **386**, 342 (2004).
[15] J. L. Delgado, P. de la Cruz, F. Langa, A. Urbina, J. Casado, and J. T. Lopez-Navarrete, Chem. Commun. (Cambridge) **2004**, 1734.
[16] J. L. Delgado, P. de la Cruz, A. Urbina, J. T. López Navarrete, J. Casado, and F. Langa, Carbon **45**, 2250 (2007).
[17] P. Lindner, R. P. May, and P. A. Timmins, Physica B (Amsterdam) **181**, 967972 (1992).
[18] *Structure Analysis by Small-Angle X-ray and Neutron Scattering*, edited by D. I. Svergun and L. A. Feigin (Plenum, New York, 1987).
[19] R. J. Roe, *Methods of X-Ray an Neutron Scattering in Polymer Science* (Oxford University Press, New York, 2000).
[20] B. J. Bauer, E. K. Hobbie, and M. L. Becker, Macromolecules **39**, 2637 (2006).
[21] P. G. de Gennes, *Scaling Concepts in Polymer Physics* (Cornell University Press, Ithaca, 1979).